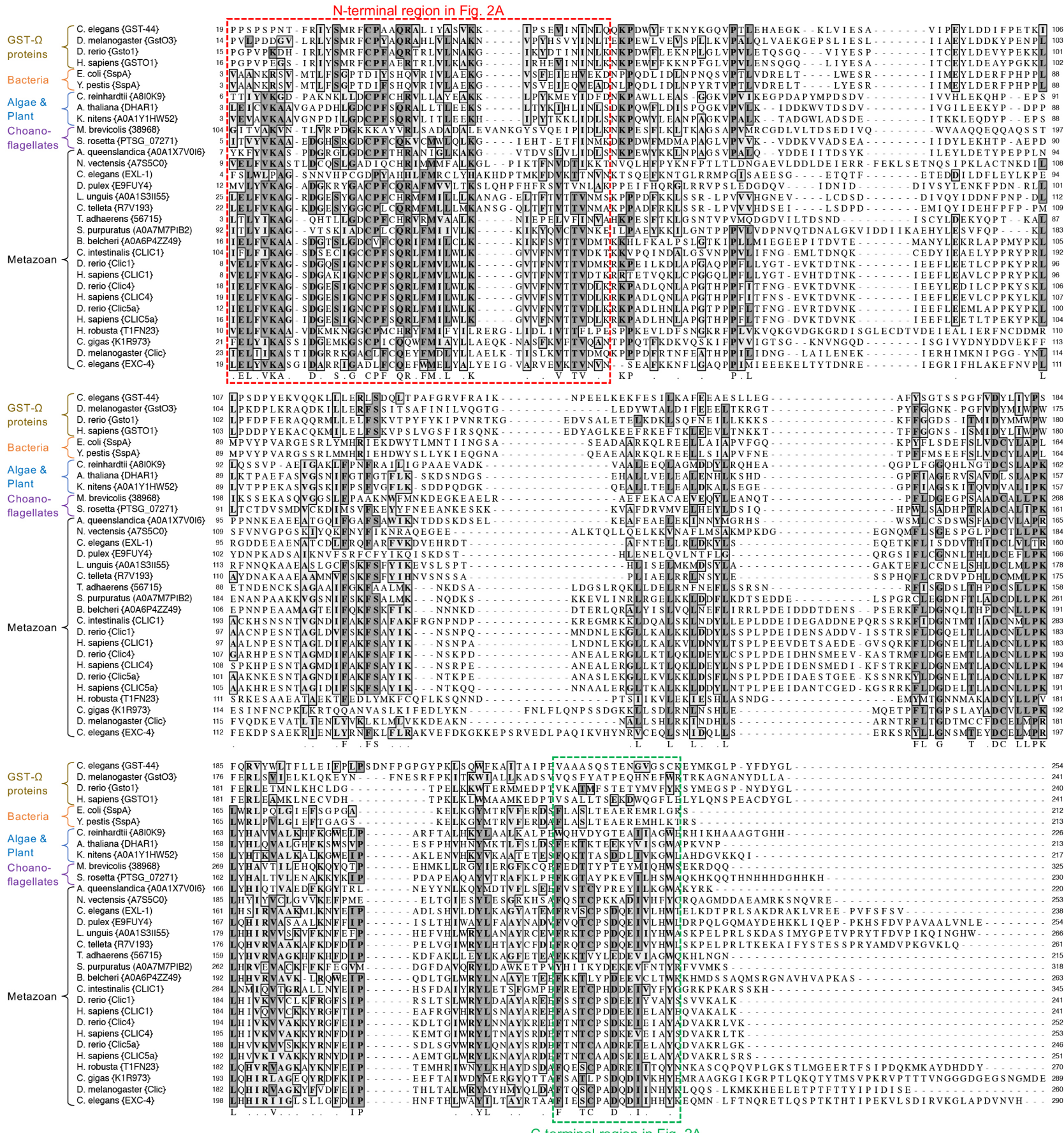
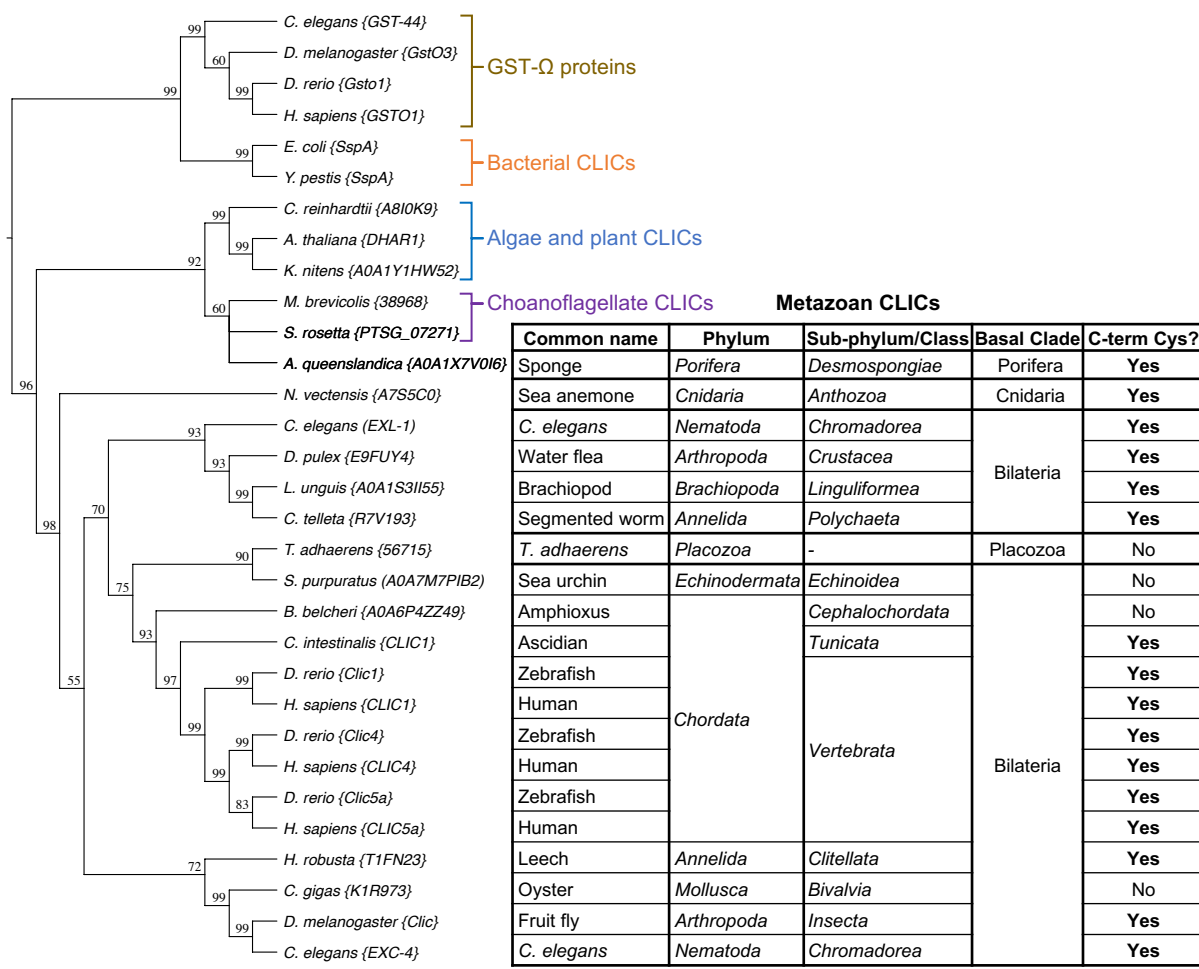


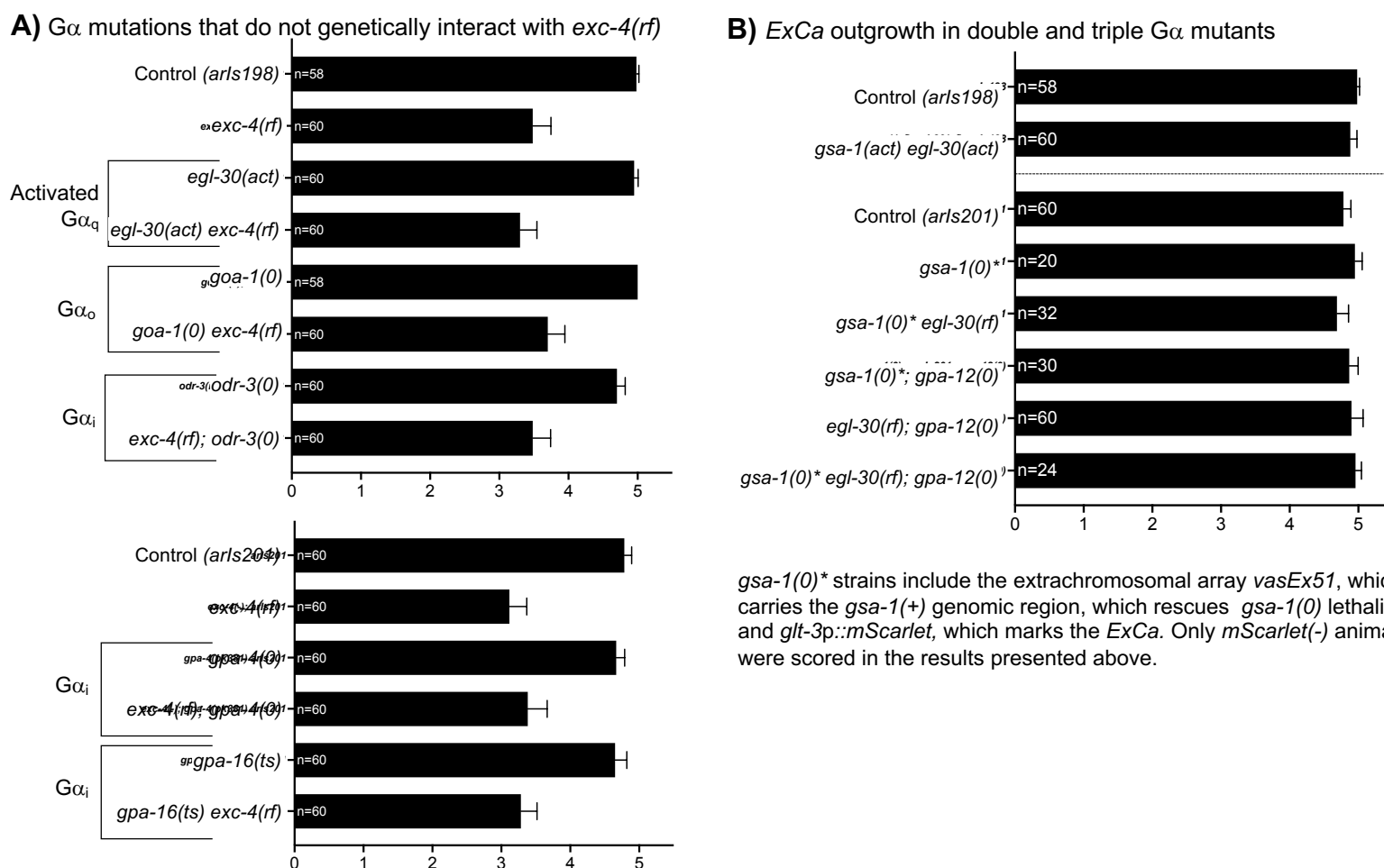
**Fig. S1. ExCa at different stages in wildtype, *exc-4(rf)*, and *exc-4(0)* animals, and *exc-4(0)* rescue by integrated multi-copy transgenes.** Nomarski and CFP fluorescence micrographs highlighting the *ExCa* in (A) wildtype, (B) *exc-4(rf)*, and (C) *exc-4(0)* at late (~3-fold) embryonic, first larval (L1), and L4 stages. Note that although areas of lumen enlargement (orange arrows) are seen in *exc-4(rf)*, we cannot conclude that these represent bona-fide cysts (red arrows) as seen in *exc-4(0)*, and in many other *ExCa* mutants (Buechner et al., 1999; Fujita et al., 2003; Gobel et al., 2004; Tong and Buechner, 2008; Mattingly and Buechner, 2011; Khan et al., 2013; Kolotuev et al., 2013; Armenti et al., 2014; Lant et al., 2015; Grussendorf et al., 2016; Al-Hashimi et al., 2018; Yang et al., 2020; Abrams and Nance, 2021), or whether these focal areas of lumen growth represent a failure to properly “resolve” varicosities/pearls (white arrows) seen during normal *ExCa* tubulogenesis and in response to physiological stresses (Hahn-Windgassen and Van Gilst, 2009; Khan et al., 2013; Kolotuev et al., 2013; Armenti et al., 2014). Scale bars = 10 $\mu$ m in embryo panels, and 50 $\mu$ m in larval stage panels. Quantifying the rescue of *exc-4(0)* outgrowth (D) and cystic (E) phenotypes by multi-copy integrated transgenes expressing EXC-4::Venus (*arl190*) or EXC-4<sup>C237Y</sup>::Venus (*vasl2*).



**Fig. S2. Full-length GST-Ω and CLIC protein alignments. (A)** CLUSTALW alignment (see Methods) of full-length GST-Ω proteins from *C. elegans*, *Drosophila*, zebrafish, and humans (brown), and CLICs from bacteria (orange), plants and algae (blue), choanoflagellate (purple), and metazoan (black). N- and C-terminal regions shown in Fig. 2 of the main text are boxed in red and green, respectively



**Fig. S3. Phylogenetic tree of GST-Ω and CLIC proteins.** Proteins from each major branch labelled in colors as described in Fig. 2A and Supplemental Fig. S2. Accepted names, or Genbank/Uniprot identifiers, are noted for each protein. The tree was rooted (not shown) to the full-length protein sequence of yeast Gtt2p (Choi et al., 1998; Ma et al., 2009), a functionally divergent GST. The % branch support shown at each branch point.



*gsa-1(0)\** strains include the extrachromosomal array *vasEx51*, which carries the *gsa-1(+)* genomic region, which rescues *gsa-1(0)* lethality, and *glt-3p::mScarlet*, which marks the ExCa. Only *mScarlet(-)* animals were scored in the results presented above.

**Fig. S4. Further genetic studies of G $\alpha$ -encoding genes.** (A) an activating mutation in *egl-30/Gα<sub>q</sub>*, or loss-of-function mutations in *goa-1/Gα<sub>o</sub>*, *odr-3/Gα<sub>i</sub>*, *gpa-4/Gα<sub>i</sub>*, or *gpa-16/Gα<sub>i</sub>*, do not cause outgrowth defects on their own, nor do they display genetic interactions with *exc-4(rf)*. (B) combining *gsa-1* and *egl-30* activating mutations, or *gsa-1(0)* (rescued for lethality by the extrachromosomal array *vasEx51*. See Supp. Methods), *egl-30(rf)* and *gpa-12(0)* double- and triple-mutants do not cause ExCa outgrowth defects. Alleles used are listed below. For full genotypes see Supplementary Table S1.

- egl-30(act) = egl-30(ep271)* (Brundage et al., 1996)
- gpa-16(ts) = gpa-16(it143)* (Bergmann et al., 2003)
- gpa-4(0) = gpa-4(pk381)* (Jansen et al., 1999)
- odr-3(0) = odr-3(n1605)* (Roayaie et al., 1998)
- goa-1(0) = goa-1(sa734)* (Robatzek and Thomas, 2000)

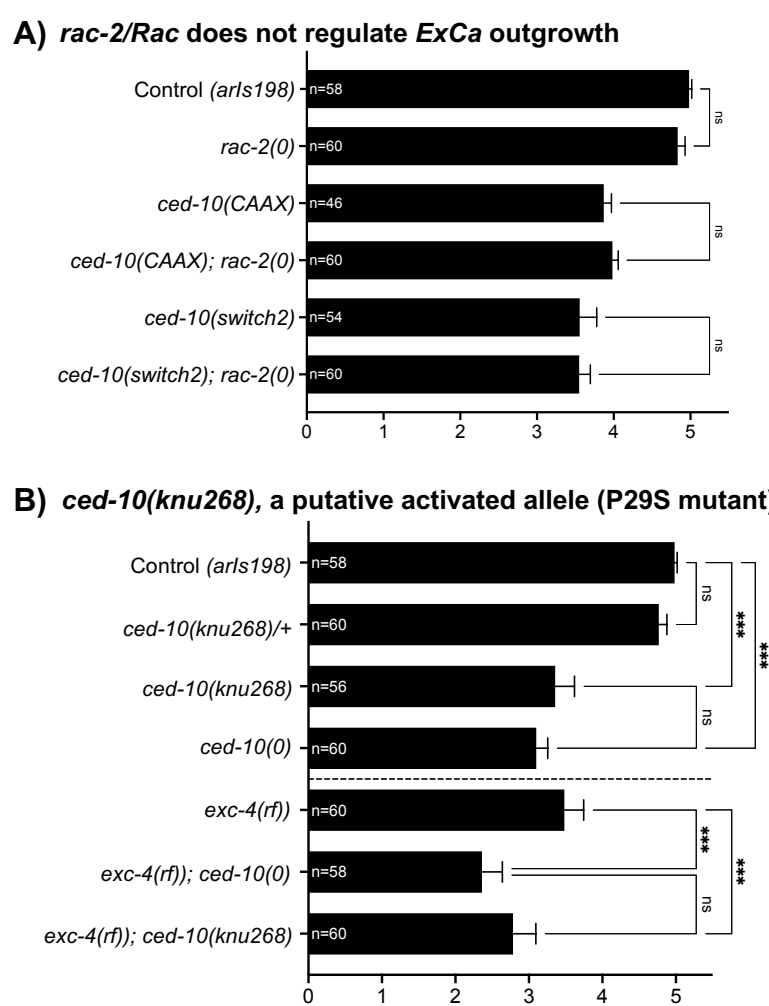


**Fig. S5. Genetic analysis of *rac-2/Rac* and *ced-10(knu268)*.** **(A)** a large genomic deletion of the *rac-2/Rac* locus, *rac-2(ok326)*, on its own, or when combined with *ced-10/Rac* loss-of-function mutations, does not affect *ExCa* outgrowth. **(B)** a putative activated *ced-10/Rac* allele, *ced-10(knu268)* with a Pro<sup>29</sup> to Ser mutation (Norgaard et al., 2018), is unexpectedly recessive for *ExCa* outgrowth defects. In addition, *ced-10(knu268)* and *ced-10(0)* mutants act in the same manner when combined with *exc-4(rf)*, raising questions as to whether *ced-10(knu268)* acts as an activated allele with respect to regulation of *ExCa* outgrowth.

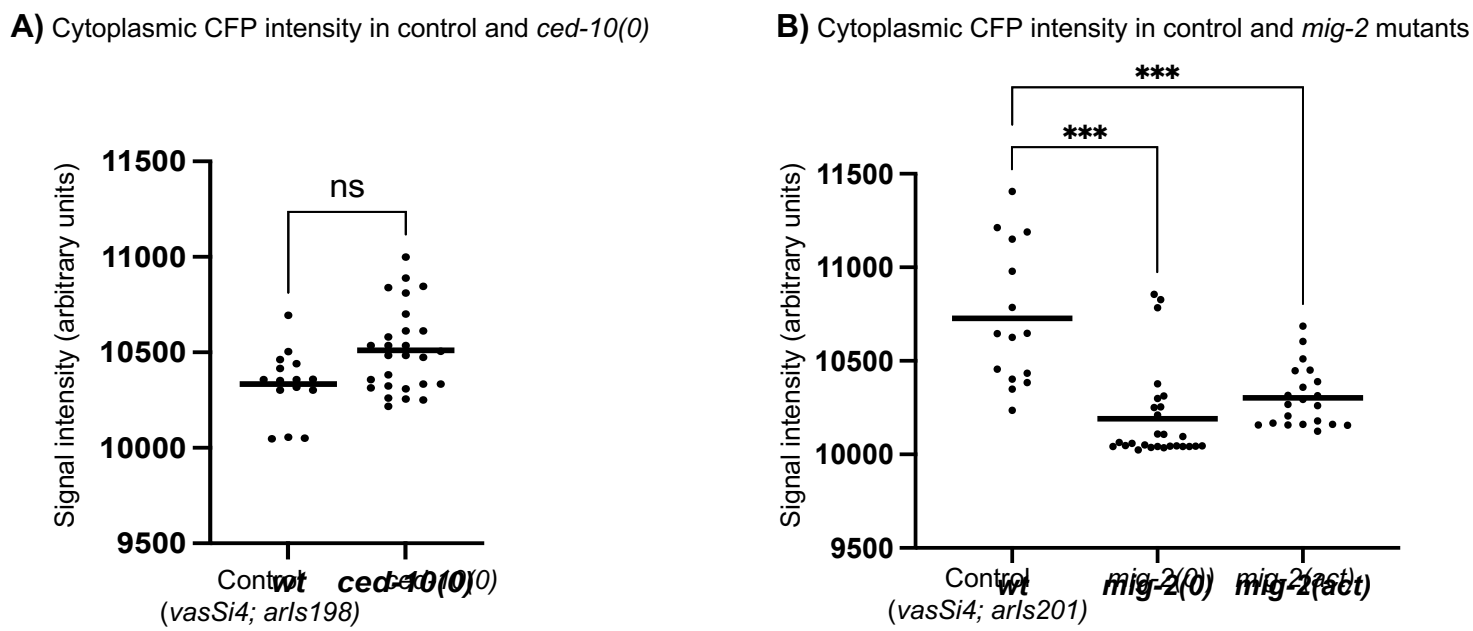


**Fig. S6. Cytoplasmic CFP levels in *ced-10* and *mig-2* mutants.** (A) to ensure that the *ced-10(0)* mutation did not affect expression from the *glt-3p* promoter, we compared overall CFP expression levels in regions-of-interest where EXC-4::Venus levels were also measured (see Fig. 5B in main text) in control and *ced-10(0)* mutants, and found that loss of *ced-10* does not significantly affect CFP expression. In contrast, *mig-2* mutations (B) significantly decrease CFP expression, indicating that these mutations may affect expression from the *glt-3p* promoter.

**Table S1. Strains and genotypes.**

[Click here to download Table S1](#)

**Table S2. Primers.** Restriction sites (underlined) and start/stop codons (bold) are shown in cDNA primers.

[Click here to download Table S2](#)

**Table S3. gBlocks.**

[Click here to download Table S3](#)

## Supplementary Materials and Methods

### **Plasmid construction**

pAA1 – *ttTi4348[SEC, MCS]*. Plasmid pWZ109 (a gift from A. Pani, D. Matus, and B. Goldstein) contains a self-excising cassette (SEC), for selection of CRISPR/Cas9-generated insertions (Dickinson et al., 2015), a TagBFP2 fluorescent reporter, and homology to the expression-permissive LG1 locus *ttTi4348* (Frokjaer-Jensen, 2015).

The TagBFP2 portion of pWZ109 was removed by NotI/AvrII digestion and replaced with annealed and phosphorylated primers oDS812 and oDS813, creating pAA1, which contains a multiple cloning site (MCS) and the SEC flanked by homology to *ttTi4348*.

pAA8 – *ttTi4348[SEC, glt-3p::Venus]*. Plasmid pDS242, encoding *Venus* flanked by the *ExCa* promoter *glt-3p* and the *unc-54* 3'UTR (Shaye and Greenwald, 2015), was digested with SphI and ApaI and the *glt-3p::Venus::unc-54* 3' fragment from this digestion was cloned into SphI/ApaI digested pAA1, generating pAA8.

pAA14 – *glt-3p::exc-4::Venus*. The *exc-4* cDNA was previously PCR amplified and Gateway cloned into pDONR221 (Invitrogen) to make pDS323 (D. Shaye, unpublished). The *exc-4* cDNA from pDS323 was PCR amplified with oDS774 and oDS775. This PCR product was digested with AgeI/BspI and cloned into AgeI/BspI-digested pDS242 to create pAA14.

pAA15 – *glt-3p::exc-4<sup>C237Y</sup>::Venus*. Using pAA14 as a template we performed two PCR reactions with primer pairs oDS37/oAA6 and oAA7/oDS40 to generate fragments with a 33bp overlap (bp 694-726 of *exc-4* cDNA). Primers oAA6 and oAA7 change the sequence <sup>709</sup>TGT·CCC·GCC<sup>717</sup>, encoding Cys<sup>237</sup>-Pro-Ala, to TAT·CCT·GCA, encoding Tyr<sup>237</sup>-Pro-Ala and a *PstI* site. These fragments were used as templates in a second round of PCR, with primers oDS37 and oDS40, to obtain a “fused” fragment that was digested with AgeI and BspI and ligated into AgeI/BspI-digested pDS242, making pAA15.

pAA23 – *Neo<sup>R</sup>-miniMos [glt-3p::Gibson::unc-54 3'UTR]*. To avoid high levels of Rho GTPase expression, and possible associated pleiotropies, we wanted to make single-copy transgenes carrying *glt-3p*-driven *ced-10* and *mig-2* cDNAs. Plasmid pCFJ910 (a gift from Erik Jorgensen, Addgene plasmid # 44481), which contains a neomycin-resistant (*Neo<sup>R</sup>*) “mini” Mos1 transposon used to generate randomly-inserted single-copy transgenes (Frokjaer-Jensen et al., 2014), was digested with SnaBI and StuI, and the GeneBlock gAA3 (IDT) was introduced via Gibson assembly (Gibson et al., 2009). The resulting plasmid, pAA23, encodes a *Neo<sup>R</sup>-miniMos* transposon with a unique restriction site (XmaI) flanked by 50 to 60 bp of homology to the 5' end of the *glt-3* promoter and the 3' end of the *unc-54* 3'UTR. Thus, we can excise *glt-3p*-driven and *unc-54* 3'UTR-containing constructs from their original backbones and efficiently Gibson-clone them into XmaI-digested pAA23 to create *Neo<sup>R</sup>-miniMos* constructs to generate Mos-mediated random single-copy transgene insertions.

pAA42 – *Neo<sup>R</sup>-miniMos[glt-3p::FLAG::ced-10]*. The *ced-10* cDNA was PCR amplified with primers oDS1067 and oDS1068, adding an N-terminal FLAG in frame to *ced-10*. This PCR product was digested with XmaI and

NotI and inserted into AgeI/NotI-digested pDS242 to generate plasmid pJE13. This plasmid was then digested with SphI/SpeI to release the *glt-3p::FLAG::ced-10::unc-54 3'UTR* fragment, which was then Gibson cloned into XmaI-digested pAA23 to generate pAA42.

**pAA54 – *glt-3p::wrmscarlet-I::3xFLAG::ced-10*.** A *C. elegans*-optimized version of the red fluorescent protein mScarlet-I (El Mouridi et al., 2017) was PCR amplified from plasmid pJE22 [*glt-3p::wrmscarlet-I*. D. Shaye, J. Escudero, unpublished] with primers oAA78 and oAA79, which include >20bp of homology flanking a unique BamHI site in plasmid pAA48 [*glt-3p::3XFLAG::ced-10*. D. Shaye, A. Arena, unpublished]. The PCR product was Gibson cloned (Gibson et al., 2009) into BamHI-digested pAA48, resulting in plasmid pAA54.

**pJE24 – *ttTi4348[FRT-HygroR::let-858-FRT/glt-3p::MCS::unc-54'3UTR]*.** Plasmid pAA1 (described above) was digested with KpnI, NheI, and MluI to remove the Self-excising cassette (SEC). Plasmid pIR98, which carries a Hygromycin resistance (HygroR) cassette (Radman et al., 2013) was cut with KpnI, SpeI, and XmaI, and the KpnI/SpeI fragment, carrying the HygroR cassette was excised. The KpnI/NheI backbone of pAA1 was ligated to the KpnI/SpeI HygroR fragment from pIR98. The resulting plasmid was next cut with XbaI/XmaI, releasing a 233bp fragment between the *ttTi4348* “left” homology arm and the HygroR promoter, and with NheI/PstI, releasing a 109bp fragment between the 3'UTR of the HygroR cassette and the “right” *ttTi4348* homology arm. gBlocks gbDS1\* and gbDS2\*, encoding FRT sequences with homology to the 5' and 3' ends of the HygroR cassette respectively, were Gibson cloned into the digested plasmid, resulting in construct pAS117 (A. Socovich and D. Shaye, unpublished), carrying a HygroR cassette that can be removed by FLP/FRT-mediated recombination (Voutev and Hubbard, 2008). We found that the *unc-54* 3'UTR of the HygroR cassette interfered with our ability to Gibson clone constructs of interest, which also carry the *unc-54* 3'UTR, into pAS117. Therefore, we replaced the *unc-54* 3'UTR in pAS117 with the *let-858* 3'UTR by Gibson cloning gBlock gJE5, resulting in plasmid pJE24, which was used as a backbone to introduce constructs of interest into the *ttTi4348* site in LG1 via MosSCI (Frokjaer-Jensen, 2015).

**pJE43 – *ttTi4348[FRT-HygroR::let-858-FRT/glt-3p::exc-4::Venus]*.** Plasmid pAA14 (described above) was digested with SpeI, SphI, and PvuI to release the *glt-3p::exc-4::Venus* fragment, which was cloned into SpeI/SphI-digested pJE24.

**pJE51 – *ttTi4348[FRT-HygroR::let-858-FRT/glt-3p::exc-4(opt)]*.** gBlock gbDS7 is a dsDNA gBlock encoding a codon-optimized *exc-4* cDNA with a synthetic intron was purchased from IDT and Gibson cloned into EcoRV+NheI digested pDS242 (*glt-3p::Venus*, described above). The resulting *virus::exc-4(opt)* plasmid, pJE48, was then digested with AgeI+NgoMIV, to release the *virus* sequence, and re-ligated to generate pJE50;

a plasmid encoding untagged *glt-3p::exc-4(opt)::unc-54 3'UTR*. This plasmid was then digested with SpeI, SphI, and PvuI to release the *glt-3p::exc-4(opt)* fragment, which was then ligated into SpeI/SphI-digested pJE24.

**pAA70 – *ttTi4348[FRT-HygroR::let-858-FRT/glt-3p::exc-4<sup>C237Y</sup>(opt)]*.** We used primers oDS1218 and oDS1219 and the NEB Q5 site-directed mutagenesis kit on plasmid pJE50 to introduce the C237Y mutation into *exc-4(opt)*. The resulting plasmid was sequenced, and digested with SpeI, SphI, and PvuI to release the *glt-3p::exc-4<sup>C237Y</sup>(opt)* fragment, which was then ligated into SpeI/SphI-digested pJE24.

## Supplementary References

- Abrams, J. & Nance, J.** (2021). A polarity pathway for exocyst-dependent intracellular tube extension. *Elife*, **10**.
- Al-Hashimi, H., Hall, D. H., Ackley, B. D., Lundquist, E. A. & Buechner, M.** (2018). Tubular Excretory Canal Structure Depends on Intermediate Filaments EXC-2 and IFA-4 in *Caenorhabditis elegans*. *Genetics*, **210**, 637-652.
- Armenti, S. T., Chan, E. & Nance, J.** (2014). Polarized exocyst-mediated vesicle fusion directs intracellular lumenogenesis within the *C. elegans* excretory cell. *Developmental Biology*, **394**, 110-121.
- Bergmann, D. C., Lee, M., Robertson, B., Tsou, M. F., Rose, L. S. & Wood, W. B.** (2003). Embryonic handedness choice in *C. elegans* involves the Gα protein GPA-16. *Development*, **130**, 5731-40.
- Brundage, L., Avery, L., Katz, A., Kim, U. J., Mendel, J. E., Sternberg, P. W. & Simon, M. I.** (1996). Mutations in a *C. elegans* Gqα gene disrupt movement, egg laying, and viability. *Neuron*, **16**, 999-1009.
- Buechner, M., Hall, D. H., Bhatt, H. & Hedgecock, E. M.** (1999). Cystic canal mutants in *Caenorhabditis elegans* are defective in the apical membrane domain of the renal (excretory) cell. *Dev Biol*, **214**, 227-241.
- Choi, J. H., Lou, W. & Vancura, A.** (1998). A novel membrane-bound glutathione S-transferase functions in the stationary phase of the yeast *Saccharomyces cerevisiae*. *J Biol Chem*, **273**, 29915-22.
- Dickinson, D. J., Pani, A. M., Heppert, J. K., Higgins, C. D. & Goldstein, B.** (2015). Streamlined Genome Engineering with a Self-Excising Drug Selection Cassette. *Genetics*, **200**, 1035-49.
- El Mouridi, S., Lecroisey, C., Tardy, P., Mercier, M., Leclercq-Blondel, A., Zariohi, N. & Boulin, T.** (2017). Reliable CRISPR/Cas9 Genome Engineering in *Caenorhabditis elegans* Using a Single Efficient sgRNA and an Easily Recognizable Phenotype. *G3 (Bethesda)*, **7**, 1429-1437.
- Frokjaer-Jensen, C.** (2015). Transposon-Assisted Genetic Engineering with Mos1-Mediated Single-Copy Insertion (MosSCI). *Methods Mol Biol*, **1327**, 49-58.
- Frokjaer-Jensen, C., Davis, M. W., Sarov, M., Taylor, J., Flibotte, S., Labella, M., Pozniakovsky, A., Moerman, D. G. & Jorgensen, E. M.** (2014). Random and targeted transgene insertion in *Caenorhabditis elegans* using a modified Mos1 transposon. *Nat Methods*, **11**, 529-34.
- Fujita, M., Hawkinson, D., King, K. V., Hall, D. H., Sakamoto, H. & Buechner, M.** (2003). The role of the ELAV homologue EXC-7 in the development of the *Caenorhabditis elegans* excretory canals. *Dev Biol*, **256**, 290-301.
- Gibson, D. G., Young, L., Chuang, R. Y., Venter, J. C., Hutchison, C. A., 3rd & Smith, H. O.** (2009). Enzymatic assembly of DNA molecules up to several hundred kilobases. *Nat Methods*, **6**, 343-5.
- Gobel, V., Barrett, P. L., Hall, D. H. & Fleming, J. T.** (2004). Lumen morphogenesis in *C. elegans* requires the membrane-cytoskeleton linker *erm-1*. *Dev Cell*, **6**, 865-73.
- Grussendorf, K. A., Trezza, C. J., Salem, A. T., Al-Hashimi, H., Mattingly, B. C., Kampmeyer, D. E., Khan, L. A., Hall, D. H., Gobel, V., Ackley, B. D. & Buechner, M.** (2016). Facilitation of Endosomal Recycling by an IRG Protein Homolog Maintains Apical Tubule Structure in *Caenorhabditis elegans*. *Genetics*, **203**, 1789-806.

- Hahn-Windgassen, A. & Van Gilst, M. R.** (2009). The *Caenorhabditis elegans* HNF4α Homolog, NHR-31, Mediates Excretory Tube Growth and Function through Coordinate Regulation of the Vacuolar ATPase. *PLoS Genet*, **5**, e1000553.
- Jansen, G., Thijssen, K. L., Werner, P., Van Der Horst, M., Hazendonk, E. & Plasterk, R. H.** (1999). The complete family of genes encoding G proteins of *Caenorhabditis elegans*. *Nat Genet*, **21**, 414-9.
- Khan, L. A., Zhang, H., Abraham, N., Sun, L., Fleming, J. T., Buechner, M., Hall, D. H. & Gobel, V.** (2013). Intracellular lumen extension requires ERM-1-dependent apical membrane expansion and AQP-8-mediated flux. *Nat Cell Biol*, **15**, 143-56.
- Kolotuev, I., Hyenne, V., Schwab, Y., Rodriguez, D. & Labouesse, M.** (2013). A pathway for unicellular tube extension depending on the lymphatic vessel determinant Prox1 and on osmoregulation. *Nat Cell Biol*, **15**, 157-68.
- Lant, B., Yu, B., Goudreault, M., Holmyard, D., Knight, J. D., Xu, P., Zhao, L., Chin, K., Wallace, E., Zhen, M., Gingras, A. C. & Derry, W. B.** (2015). CCM-3/STRIPAK promotes seamless tube extension through endocytic recycling. *Nat Commun*, **6**, 6449.
- Ma, X. X., Jiang, Y. L., He, Y. X., Bao, R., Chen, Y. & Zhou, C. Z.** (2009). Structures of yeast glutathione-S-transferase Gtt2 reveal a new catalytic type of GST family. *EMBO Rep*, **10**, 1320-6.
- Mattingly, B. C. & Buechner, M.** (2011). The FGD homologue EXC-5 regulates apical trafficking in *C. elegans* tubules. *Dev Biol*, **359**, 59-72.
- Norgaard, S., Deng, S., Cao, W. & Pocock, R.** (2018). Distinct CED-10/Rac1 domains confer context-specific functions in development. *PLoS Genet*, **14**, e1007670.
- Radman, I., Greiss, S. & Chin, J. W.** (2013). Efficient and rapid *C. elegans* transgenesis by bombardment and hygromycin B selection. *PLoS One*, **8**, e76019.
- Roayaie, K., Crump, J. G., Sagasti, A. & Bargmann, C. I.** (1998). The Gα Protein ODR-3 Mediates Olfactory and Nociceptive Function and Controls Cilium Morphogenesis in *C. elegans* Olfactory Neurons. *Neuron*, **20**, 55-67.
- Robatzek, M. & Thomas, J. H.** (2000). Calcium/calmodulin-dependent protein kinase II regulates *Caenorhabditis elegans* locomotion in concert with a G(o)/G(q) signaling network. *Genetics*, **156**, 1069-82.
- Shaye, D. D. & Greenwald, I.** (2015). The disease-associated formin INF2/EXC-6 organizes lumen and cell outgrowth during tubulogenesis by regulating F-actin and microtubule cytoskeletons. *Dev Cell*, **32**, 743-55.
- Tong, X. & Buechner, M.** (2008). CRIP homologues maintain apical cytoskeleton to regulate tubule size in *C. elegans*. *Dev Biol*, **317**, 225-233.
- Voutev, R. & Hubbard, E. J. A.** (2008). A "FLP-Out" System for Controlled Gene Expression in *Caenorhabditis elegans*. *Genetics*, **180**, 103-119.
- Yang, Z., Mattingly, B. C., Hall, D. H., Ackley, B. D. & Buechner, M.** (2020). Terminal web and vesicle trafficking proteins mediate nematode single-cell tubulogenesis. *J Cell Biol*, **219**.